Case Study

Three Most Widely Used GNSS-Based Shoreline Monitoring Methods to Support Integrated Coastal Zone Management Policies

R. M. Goncalves, Ph.D.[1]; and J. L. Awange, Ph.D.[2]

Abstract: Shoreline monitoring is essential for integrated coastal zone management (ICZM). It provides the necessary information needed to manage the settlement of coastal areas, establishes guidelines for management of socioeconomic activities within the coastal areas, provides information necessary for recovery actions of beach regeneration, and provides a reference baseline for studies related to climate change in coastal zones. Shoreline monitoring methods are largely dependent on goals, costs, implementation, and applicability. For monitoring of short coastal shorelines (e.g., tens to hundreds of kilometers), global navigation satellite system (GNSS)-based methods are emerging as low-cost approaches that offer rapid, weather-independent, and quickly updatable products that could benefit policy makers when high costs of traditional methods, such as photogrammetry and remote sensing, are of concern. However, various GNSS methods applicable to shoreline monitoring exist, making it difficult for decision makers to choose a suitable approach. Using a case study of the Pernambuco State ICZM in Brazil, this study evaluates three of the most commonly used GNSS-based shoreline monitoring methods, that is, relative kinematic (RK), real-time kinematic (RTK), and precise point positioning (PPP) methods. It also provides a comprehensive analysis of their strengths and limitations. The results highlight the issues and important considerations in choosing an economically viable GNSS method for mapping shoreline changes, particularly for supporting ICZM policies. **DOI: 10.1061/(ASCE)SU.1943-5428.0000219.**

Author keywords: Integrated coastal zone management (ICZM); Global navigation satellite systems (GNSS); Precise point positioning (PPP); Real-time kinematic (RTK); Relative kinematic (RK); Shoreline; Coastal monitoring.

Introduction

Coastal zones are extremely important for countries with highly populated coastal areas. Consequently, there is concern about their future, particularly on the state of their natural resources, which provide life support and opportunities for economic development and tourism for these countries (Clarck 1992). However, one of the main environmental problems facing coastal areas the world over is that of coastal erosion, which includes beach erosion and other natural and anthropogenic environmental factors that are present along the shoreline. Anthropogenic factors include settlement near the shore, which aggravates the situation, as exemplified in the case of Brazil in which hundreds of beaches are under severe erosion (Souza 2009). One way to efficiently accomplish coastal management, therefore, is to invest in monitoring of shorelines to support policy formulations.

Continuous monitoring of coastal zones is important for integrated coastal zone management (ICZM) to support informed decisions on policies governing coastal development (Boak and Turner 2005; Baldock et al. 2014; Jacobson et al. 2014; Botero et al. 2015). For example, the State of Pernambuco in Brazil established a coastal management policy through legislation (i.e., Law No. 14.258 December 23th, 2010, Pernambuco), which has an overarching policy of guiding the use of the natural resources of the Pernambuco State Coastal Zone. Among other things, this law aims to

1. Promote the development of monitoring activities of natural resources and settlement of the coastal zone;
2. Promote recovery actions and regeneration of beaches;
3. Promote the integration of the coastal management information system with other state systems of environment, water resources, and land use; and
4. Promote and support training for coastal zone municipality staff to strengthen the urban environmental control.

The four itemized components of the legislation mentioned previously require some sort of shoreline monitoring, which is essential to consistently organize the set of positional data that represents the evolution of a particular case. The four itemized components of the legislation mentioned previously require some sort of shoreline monitoring, which is essential for consistently organizing the set of positional data that represent the evolution of a particular case. There are many advantages to having shoreline-mapped data sets. Among them are the importance of providing input for review plans and coastal works, maintenance of coastal defenses, biodiversity action plans, coastal zone directives, and management.

Starting in the 1920s, it was demonstrated that great efficiency gains in shoreline mapping could be realized by transitioning from ground-based methods (e.g., plane tables, alidades, stadia rods) to airborne methods (e.g., photogrammetry and aerial imagery interpretation) (Smith 1981; Graham et al. 2003; Parrish et al. 2005; Parrish 2012). Beginning in the 1970s, when earth observation satellite data became publicly available, further gains in shoreline

[1]Associate Professor, Dept. of Cartographic Engineering, Federal Univ. of Pernambuco (UFPE) Geodetic Science and Technology of Geoinformation Post Graduation Program, Av. Academico Helio Ramos, s/n - 2° andar, Recife-PE 50740-530, Brazil (corresponding author). ORCID: http://orcid.org/0000-0002-5066-1910. E-mail: rodrigo.mikosz@ufpe.br

[2]Associate Professor, Western Australian Centre for Geodesy and Institute for Geoscience Research, Curtin Univ., GPO Box U1987, Perth, WA 6845, Australia, E-mail: J.Awange@curtin.edu.au

Note. This manuscript was submitted on April 6, 2016; approved on November 9, 2016; published online on February 27, 2017. Discussion period open until July 27, 2017; separate discussions must be submitted for individual papers. This paper is part of the ***Journal of Surveying Engineering***, © ASCE, ISSN 0733-9453.

mapping efficiency were enabled (Dolan and Heywood 1976). Today, photogrammetry, airborne lidar, and satellite imagery are well-established methods of mapping large stretches of shoreline in many areas around the world (Stockdon et al. 2002; Graham et al. 2003; White et al. 2011; Yao et al. 2015). Additionally, unmanned aerial vehicles and structure from motion are also emerging as viable coastal mapping techniques (Westoby et al. 2012; Mancini et al. 2013). However, although the cost per linear kilometer of shoreline data acquisition will generally be lowest for satellites and then followed by aircraft, there are a number of important benefits to ground-based shoreline mapping surveys. First, for very small project sites, the total acquisition cost can actually be lower using ground-based methods than for airborne methods. Second, ground-based shoreline surveys typically provide the highest accuracy, as well as the most detailed knowledge obtained by *boots on the ground*. Therefore, ground-based surveys can provide reference data for calibrating and validating airborne and spaceborne shoreline mapping techniques. Third, when shoreline data with high temporal resolution (i.e., short repeat survey periods) are needed, ground-based methods may be the best option.

When and where ground-based survey methods are advantageous for shoreline mapping, a global navigation satellite system (GNSS) is generally the technology of choice, because it has the advantages of being quicker, all weather, highly accurate, and capable of generating continuously updatable shoreline positional time series relevant for monitoring and management tasks undertaken by engineers and coastal authorities in cases of extremely small project sites that are located close to a field office and easily accessible. For such small projects the use of traditional remote sensing–based satellite techniques could be costly, although this does not apply to all cases. Furthermore, as exemplified by the National Oceanic and Atmospheric Administration (NOAA) National Geodetic Survey Coastal Mapping Program (NOAA 2017), field-based GNSS shoreline surveys are sometimes performed to obtain high-accuracy reference data for evaluating airborne or spaceborne shoreline mapping methods (White et al. 2011; Parrish et al. 2005).

GNSS comprising the use of the U.S.-based global positioning system (GPS), Russia's global navigation satellite system (GLONASS), Europe's Galileo, and China's Beidou (or Compass) (Awange 2012) have already been proposed for shoreline monitoring by Goncalves et al. (2012b). However, with a large number of types of GNSS surveys, ranging from static surveys to real-time kinematic (RTK), network real-time kinematic, postprocessed kinematic (PPK), and precise point positioning (PPP), the coastal zone management (CZM) community needs information on which types of GNSS surveys are most advantageous for shoreline mapping across a range of project types and coastal morphologies. To this end, this case study seeks to empirically compare different GNSS survey methods in a study site along the coast of Pernambuco in northeastern Brazil. Three common types of GNSS surveys (PPK, RTK, and PPP) are evaluated, and the results are compared.

The remainder of the study is organized as follows. Next, the authors discuss how shoreline mapping supports ICZM policies before considering the three GNSS-based shoreline monitoring methods and their characteristics. Then a case study of the Pernambuco State in Brazil is presented together with the data and evaluation methods used. This is followed by a discussion of the results, before concluding the study.

Mapping in Support of ICZM Policies

Shoreline mapping has widely supported ICZM plans and policies. For instance, Dibajnia et al. (2012) presented a national shoreline management plan (SMP) to the Ports and Maritime Organization of Iran that is useful for addressing existing coastal problems and setting policies that show shoreline management is the part of the ICZM policy dealing with existing and planned development in coastal areas. Although the concept of shoreline mapping supporting policy formulation is widely accepted by the ICZM community, many municipalities still use a one-size-fits-all approach to regulate oceanfront development by restricting construction to preset distances from the shoreline (Genz et al. 2009). Such a one-size-fits-all policy was shown by Abbott (2013) to have created a setback in Maui, Hawaii.

Shoreline flooding, erosion hazards, and land-use planning policies receive information from different sources and services related to erosion and flood-risk mapping. Funding for shoreline projects, access to the geographical information system database, and technical assistance are reported as the components fundamental for a SMP, as evidenced by the case study presented on the Ontario Great Lakes in Canada by Lawrence (1995).

The authors' contribution looks at the State of Pernambuco in Brazil, in which a coastal management policy was established through legislation (i.e., Law No. 14.258 December 23th, 2010, Pernambuco). Chapter V of this policy highlights the general guidelines for coastal zone settlement. Here, we describe Article 10, §2, §3, and final provisions and transitional item III as defined in Chapter VII, and assess how the three GNSS techniques for shoreline mapping and monitoring discussed in the next section could be useful in supporting this policy. Article 10 of the Pernambuco legislation reads as follows:

1. Article 10: The beaches are public goods for common use, and together with the sea are guaranteed free and unimpeded access from any direction and sense, except for the sections considered to be of public interest and national security, or included in protected areas by specific legislation.
2. §2: For urbanized areas, no new construction, installation, urbanization or any form of land use within the coastal zone will be allowed in the range of 33 m from the shoreline. This specification is considered *non aedificandi* or higher value when recommended by technical study, measured perpendicularly towards the continent from a line defined by the maximum current high spring tides, unless determined to greater or smaller extent by municipal legislation.
3. §3: For non-urbanized areas, the settlement within the range of 33 m to 100 m from the current high spring tide line will be preceded by a technical study. For defining the limit of protection, a minimum distance for *non aedificandi* as defined in paragraph 2 is always considered.
4. Chapter VII final provisions and transitional item III: Determine the maximum high tide line of the current spring tide and its monitoring within up to 3 years, for the purpose of defining the area *non aedificandi* established in Art. 10 of this Law.

From Article 10 above, it is clear that the shoreline position (items §2 and §3) is essential for the ranges, i.e., 33 m in §2 and 33–100 m in §3, to be realized. In Chapter VII, it is also noted that the position of the spring tide is required and needs to be monitored every 3 years. All these calls for shoreline monitoring are discussed in the next section (Fig. 1).

GNSS Shoreline Monitoring and Mapping

The sea is dominated by waves and also by tidal responses of the ocean to forcing produced by the attraction of the moon and the sun. Tides are mainly responsible for the periodicity mark. The main

tidal features of a tidal level record are the range, measured as the height between successive high and low levels, and the period, the time between the high (or low) level and the next high (or low level). For the case of semidiurnal tides, each tidal cycle takes an average of 12 h 25 min; thus, two tidal cycles occur for each transit of the moon (every 24 h 50 min). High tides occur in most localities twice daily and are about 50 min later on the successive day. The maximum ranges, called spring tides, occur a few days after both new and full moons (or syzygy, when the moon, the Earth, and the sun are in line), whereas the minimum ranges, called neap tides, occur shortly after the times of the first and last quarters (lunar quadrature) (Pugh 1987).

Fig. 1 represents some shoreline indicators in a coastal profile. The mean high water and mean low water both take into account a tidal datum defined by the intersection of the coastal profile with a special vertical elevation defined by the tidal constituents of a particular beach. The same case applies to the spring tide line, which by definition is dependent on a specific epoch related to the tide. Fig. 1 also represents the vegetation line, dune, berm, beach face, and wet beach. For the ICZM policy of Pernambuco State, for example, it is desirable to map the spring tide line and, based on this limit, to build a buffer zone as *non aedificandi* (see a GNSS receiver mapping of this boundary). Notice that a spring tide line position is not fixed during time and is also dependent on sediment transport and geomorphological characteristics of a beach that can be affected by climate change and anthropogenic factors. This fact highlights the importance of monitoring its position. In the following sections, three commonly used GNSS positioning techniques [relative kinematic (RK), RTK, and PPP] are discussed with examples on how they can be used to map the spring tide line in Fig. 1 elucidated.

RK

The basic concept of RK positioning is to determine the coordinates of unknown points (e.g., the spring tide line's position as shown in Fig. 1) with respect to a known point (the station whose position is precisely known, e.g., a base or reference station) [Fig. 2(a)]. In this technique, the reference receiver at a known Station *A* remains fixed, and the second receiver (known as the roving receiver) moves collecting data that are later processed using a given vendor software, e.g., Trimble Business Center, to determine the positions. The roving receiver can be mounted on a vehicle (Fig. 3) or simply held by the observer. Although the reference station collects data during the entire period of observation, the roving receiver can collect data at a point between 5 and 10 min before moving to another point or collect kinematically. Both receivers (reference and rover) observe the same GNSS satellites simultaneously to determine a baseline, i.e., the distance between the known Point *A* and the roving receiver at a Point *B*.

The main purpose of having two receivers, one fixed and the other roving, is to enable elimination or minimization of common errors, such as satellite clock error, ionospheric delay, tropospheric delay, and ephemeris errors, among others. The advantage of this method is that it provides more accurate results compared with the RTK and PPP methods discussed next, i.e., centimeter-level accuracy. This is because it permits postobservation processing, which is a period that precise known satellite positions could be used and more errors eliminated by deselecting poor satellites. Moreover, common errors in both reference and roving stations cancel out by using baseline processing techniques during data processing. The disadvantage of the method is its reliance on two receivers, increasing the hardware and manpower costs for the authority undertaking the monitoring campaign. Furthermore, the obtained roving positions will be relative to that of the reference station due to the nature of the method, in which the baseline vector is computed and its elements added to the position of the reference station to obtain the position of the rover. Any errors in the reference station or wrong input of the reference station will propagate to the roving station, hence, impacting the shoreline determination. An example of the application of the RK method to shoreline mapping, particularly

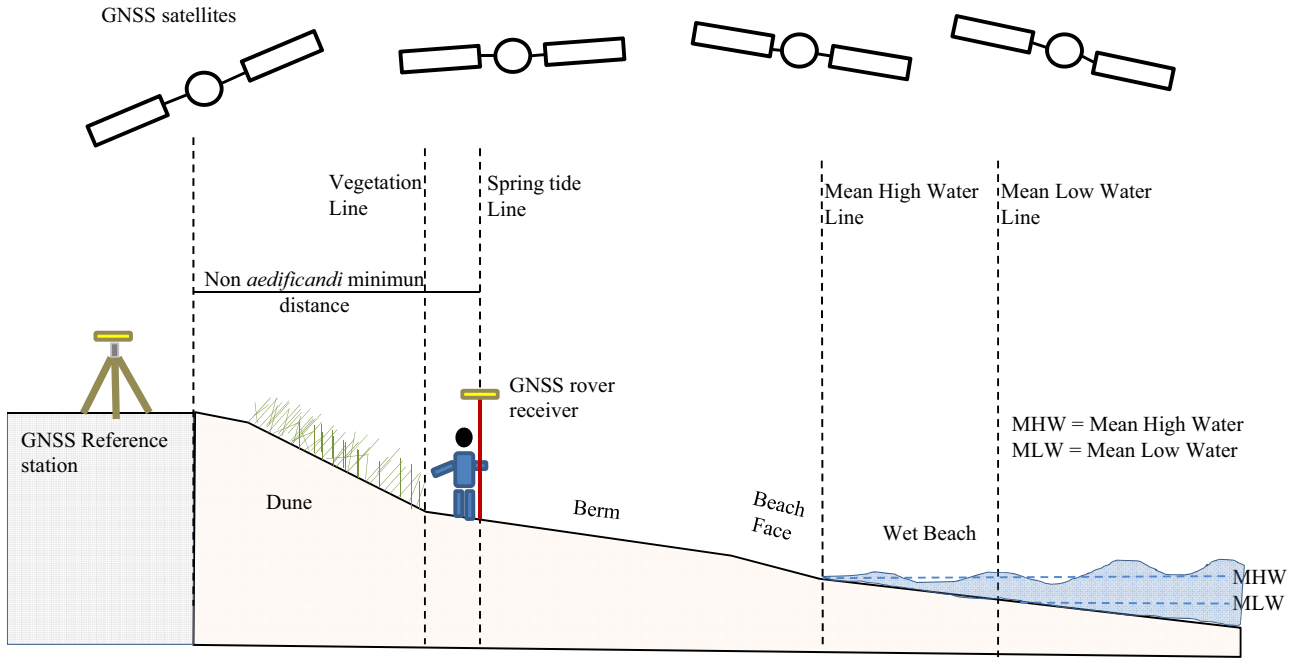

Fig. 1: GNSS reference static stations and a person with a rover receiver tracking four satellites in a beach profile with some shoreline indicators (e.g., MHW, MLW, vegetation line, and spring tide line)

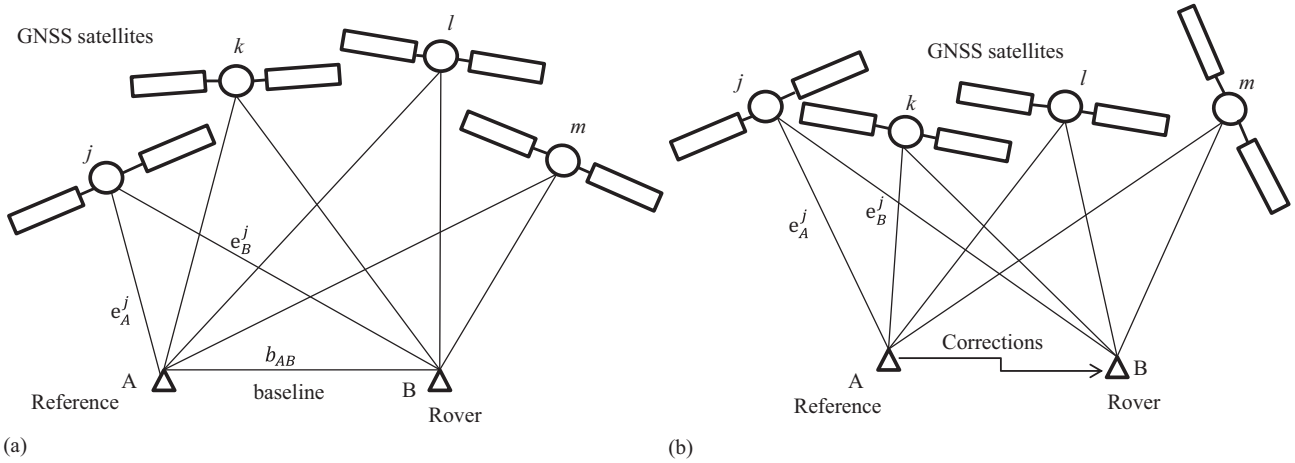

Fig. 2: (a) RK [Note: A = known reference (fixed) station; B = unknown roving station; b_{AB} = baseline; and e_A and e_B = geometric distances between the satellites and the receivers); (b) RTK method, in which the carrier phase and other information (e.g., base station coordinates and its antenna heights) are sent from Reference Receiver A attached to a radio transmitter via communication link to Roving Receiver B attached to a radio receiver; Roving Receiver B combines and processes the received data to get the coordinates of the rover [(a) and (b) adapted from Howfman-Wellenhof et al. 2008]

Fig. 3: Example of a shoreline survey using a vehicle with a GNSS receiver; the line represents the shoreline indicator mapped (image by R. M. Goncalves)

when the reference station is near the shoreline, is presented in Goncalves et al. (2012a). In Fig. 1, for example, the spring tide line position could be mapped by having a reference station fixed on the ground to the left, and the roving station mounted on a mobile device, as shown in Fig. 3. Details of the RK method can be found in Leick (2004), Howfman-Wellenhof et al. (2008), and Awange (2012).

RTK

Fig. 2(b) shows the basic configuration for the RTK method, which is considered a real-time positioning using two or more receivers. The basic configuration for this technique consists of a receiver fixed at a Point A with known coordinates and a rover at a Point B [similar to the configuration of the RK method in Fig. 2(a)]. The difference between RTK and RK methods, however, is that RTK is capable of delivering real-time positions in the field as opposed to RK, thus alleviating the need for postprocessing the data. Similar to the RK technique discussed previously, RTK also requires more than two receivers, with one placed at a reference (base station) station and both measuring carrier phases.

For RTK, the receiver at the control station attached to a radio transmitter samples data every second and transmits these raw data together with its position (along with the antenna height) via the communication link (e.g., satellites, mobile phones, radio) to the roving receiver attached to a radio receiver (Awange 2012). Using its radio receiver, the rover receives the transmitted data from the base receiver and uses its built-in software to combine and process the GNSS measurements obtained at both the base and roving receiver to obtain its position in real time (El-Rabbany 2006, p. 76). Some GNSS manufacturers provide a handheld controller that can be used to operate both the roving and the base receivers. Normally, the user carries the roving receiver attached to the radio link in a backpack. This method requires fixing the integer ambiguity at the start of the survey (initialization) before undertaking it.

One of the limitations of this method is that any loss of lock by the receivers to the satellite due to obstruction or loss of communication between the receivers could cause loss of accuracy in positioning. In addition, similar to the RK method, RTK requires the use of at least two receivers, increasing the costs. Reliance on radio link also means that the method can only be used to monitor shorter shoreline lengths in which radio communication is permissible. Furthermore, compared with RK, the quality of the obtained positions at the rover are degraded to latency (i.e., the control station data reaches the rover after some delay). Its use in monitoring the spring tide line in Fig. 1, for example, would be the same as the RK method in terms of configuration, but the roving receiver in Fig. 2(b) will provide the positions in real time (no need for

postprocessing). This method could be useful for shoreline monitoring in cases in which instant decisions are to be made in real time. Its accuracy is to the centimeter level, which is way beyond the required accuracy for shoreline mapping that in most cases ranges from decimeters to meters. The RTK method has been used in coastal applications to determine modifications in dunes by obtaining positions used to generate digital terrain models (Portz et al. 2015) and also when collecting bathymetric data of ocean bottom topography (Dugan et al. 2001).

PPP

Unlike the RTK and RK methods, PPP only needs a single GNSS receiver during the shoreline monitoring to achieve centimeter-level accuracy (static); thus, it becomes attractive for shoreline mapping in terms of reduced costs of the equipment and personnel. This accuracy is achieved by addressing the factors that bedevil the RTK and RK methods, i.e., orbital errors, clock errors, and atmospheric errors (ionosphere and troposphere) (Leandro et al. 2011; Juan et al. 2012). During postprocessing, the PPP method exploits the precise GNSS orbital and clock parameters provided, e.g., by the International GNSS Service, Jet Propulsion Laboratory, and other commercial sources (Awange 2012).

From the PPP method, it is possible to obtain the position of a station or trajectory to centimeter-level accuracy in two ways: estimation close to real time (latency in seconds) mode or postprocessing. Using the precise GNSS orbit (accurate ephemerides data), clock information products, and the dual-frequency code pseudorange and/or carrier phase observations, the PPP method processes the ionospheric-free combinations of undifferenced code and phase observations to estimate the positions, integer ambiguity N, and the tropospheric effect (Howfman-Wellenhof et al. 2008, pp. 166–169).

Its advantages compared with RK and RTK are the following (Gao 2006; Awange 2012):

1. It uses only a single receiver to achieve centimeter-level accuracy, hence, removing the requirement of a reference station and simultaneous observations to the same satellites from both the rover and the reference station. Furthermore, the operating range limit is not an issue.
2. Its use of a global reference frame gives it a global outlook enabling it to provide much greater consistency.
3. Its use of a single receiver reduces equipment cost and also makes the approach less labor intensive.
4. Along with the provision of location-based data, PPP needs to estimate clock and tropospheric effect parameters, providing a new way for precise time transfer and water-vapor estimating using a single GNSS receiver.

Its disadvantage, however, is the convergence time, which is rather long. The PPP sometimes requires around 30 min to obtain centimeter-level accuracy or to succeed in the first ambiguity fixing (Li and Zhang 2014).

Case Study: Pernambuco State in Brazil

Background of the Study Area

The coast of Pernambuco, located in the northeastern region of Brazil, has a range of 187 km of nearby shoreline bathed by the Atlantic Ocean. Pernambuco's capital, Recife, according to the Brazilian Institute of Geography and Statistics (IBGE) census (IBGE 2010), had a population of about 1.6 million within an area of approximately 218 km^2, leading to a very high population density of about 7,000 inhabitants per square kilometer. The total population living within the coastal municipalities in Pernambuco State is about 3.9 million. Pernambuco's coastal zone, with a variety of ecosystems, such as coconut trees, Atlantic forest remnants, sandbanks, estuaries, mangroves, coral reefs, and islands, among others, is divided into sectors based on their geographical locations in 21 municipalities. For management purposes, the following three sectors were delineated, as shown in Fig. 4:

1. Northern Sector, which is comprised of the municipalities Goiana, Itamaracá, Igarassu, Araçoiaba, Abreu e Lima, Paulista, Itapissuma, and Itaquitinga.
2. Metropolitan Sector, which is comprised of the municipalities Recife, Olinda, Jaboatão dos Guararapes, São Lourenço da Mata, Camaragibe, and Moreno.
3. Southern Sector, which is comprised of the municipalities Cabo de Santo Agostinho, Ipojuca, Sirinhaém, Rio Formoso, Tamandaré, Barreiros, and São José da Coroa Grande.

The coast of Pernambuco has been impacted by coastal and anthropogenic processes in recent years. Exponential population growth in this area coupled by a disorderly explosion of tourism activities precipitated changes in land use near the shoreline that increased coastal erosion processes considered irreversible in some sectors of the municipalities. Thus, the activities undertaken by coastal management in the State of Pernambuco provides subsidies for environmental and land management of the state, mainly for the activities of controlling, licensing, and environmental monitoring to improve the quality of the environment and generate socioeconomic benefits.

The 2.4-km extension used in this study belongs to the Metropolitan Sector shown in Fig. 4. Manso et al. (2006) reported that the development and expansion of Recife was mainly along the rivers and coastal zones. Over time, the beaches of Candeias, Piedade, and south of Boa Viagem, which had a stable shoreline, began to experience problems of coastal erosion believed to be related to the settlement close to the shoreline position. Temporal shoreline series analysis using GNSS in this study area can be found in more detail in Mendonça et al. (2014). Since the last decades a large rise in building construction, condominiums, and hotels along the waterfront has taken place.

The coastal zone of Recife with latitude around 8°S has an average temperature of about 27°C and approximate rainfall of 2,000 mm/year. The winds prevail in the E-SE direction with an average speed of 3–5 m/s, and there are waves with a mean height of 1.0–1.5 m in 5- to 7-s periods during most parts of the year (Manso et al. 2006; Mallmann et al. 2014). The tide range of Pernambuco State is semidiurnal (two nearly equal high and low tides each day) with a 2.0-m average of amplitude for spring tides and 0.7 for neap tides. There are also Pleistocene marine terraces (7–11 m high) and Holocene (1–5 m high) designed during the last marine transgression. In addition to swamp deposits, there are banks of sandstone or beachrocks in the study area. The beachrocks have a width average of 20–60 m and are 3–4 m in thickness. They are arranged parallel to the shoreline to protect the coast from the wave energy effect but can also generate an erosion process at their edges (Dominguez et al. 1990; Manso et al. 2006). The sediments, which comprise the studied stretch, exhibit great homogeneity and are formed by thin medium sand with an average diameter of 0.30 mm (Muehe 2006).

Shoreline Indicator Feature

According to Boak and Turner (2005), the idealized shoreline boundary and recognition require the use of a *shoreline indicator*, i.e., a feature that is used as a proxy to represent the *true* shoreline position. For the purpose of the experiment, the shoreline identified

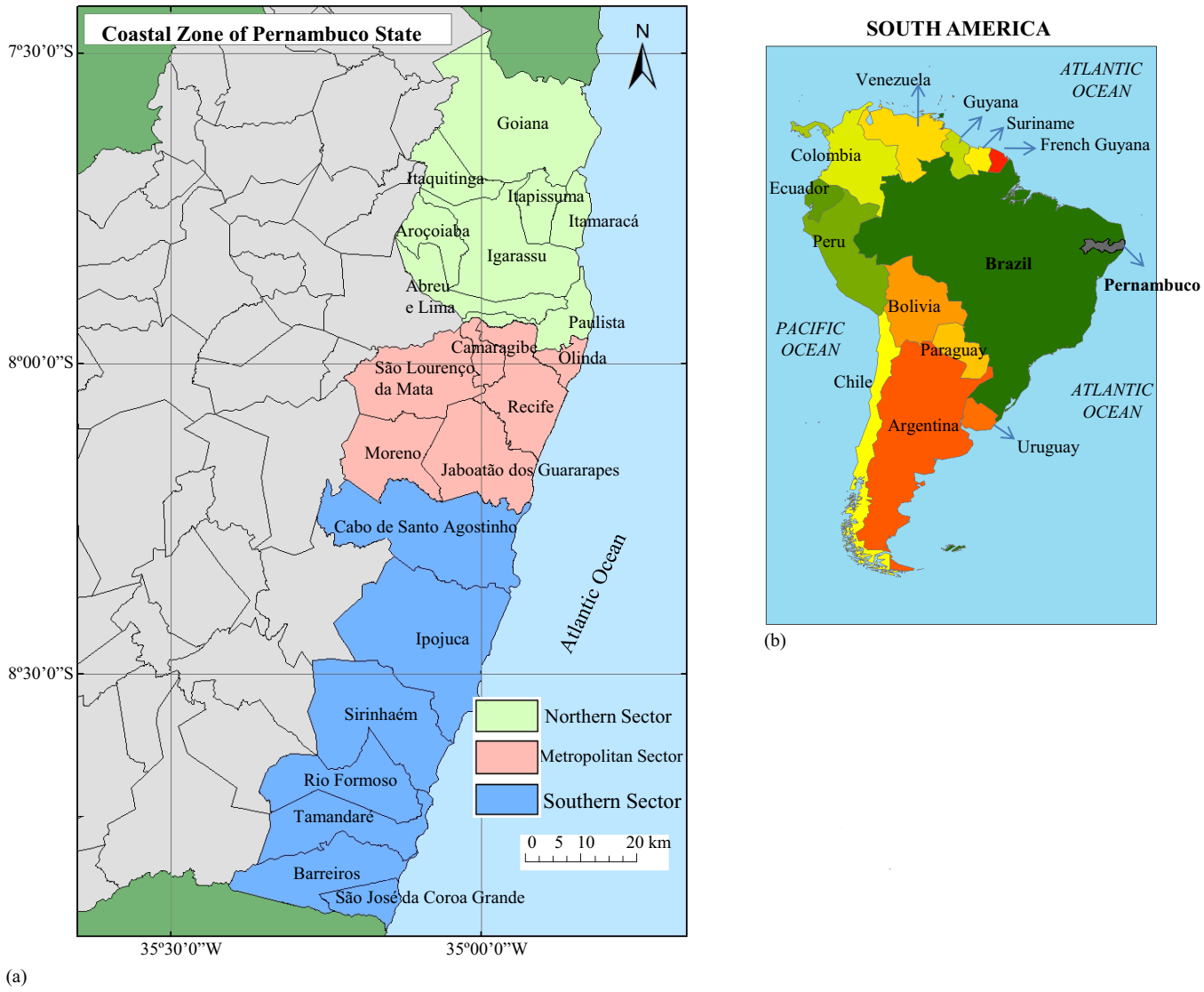

Fig. 4: Pernambuco State seashore: (a) division of Pernambuco into sectors: northern, metropolitan, and southern (the northern and southern boundaries are the municipalities of Goiana and São José da Coroa Grande, respectively); (b) localization of Pernambuco State in Brazil

in the field surveys was the border between wet and dry, and was visually interpreted by a team comprised of surveying engineering students from the Federal University of Pernambuco (UFPE) that were trained to perform the survey using the high tide of the survey day as a reference. This can be repeated anywhere for a particular time of the year using the CZM policies and mapping the desired spring tide line depicted in Fig. 1. For kinematic GNSS surveys, two sets of equipment were used, as shown in Fig. 5, and are described as Team A (undertaking RK and PPP) and Team B (undertaking RTK). After setting the equipment, Team A started to survey the shoreline indicator using the kinematic approach, and Team B followed exactly the same track collecting RTK data.

Fig. 5: Field survey: Team A taking care of PPP and RK survey and Team B undertaking the RTK survey (image by R. M. Goncalves)

RK Method: Data Collection and Processing

For this approach, the reference station was the Brazilian network for continuous monitoring (RBMC) located at the UFPE. This station is located approximately 10 km away from the shoreline under study. Data collection was conducted on January 29, 2014, with high tides used to indicate the shoreline position. Both the reference receiver at the RBMC and the roving receiver along the shoreline were set in such a way that they simultaneously logged data from the same satellites every 15 s [Fig. 2(a)]. The roving receiver (Viva

Table 1. Number of Data Collected and the Time Spent by Each Method

Method	Number of points	Distance (km)	Start time (h, min)	End time (h, min)	Time interval (min)	Velocity (km/h)
slRTK	76	—	—	—	—	—
slRK	200	2.4	14, 47	15, 37	50	2.9
slPPP	200	—	—	—	—	—

GS15, Leica Geosystems AG, Heerbrugg, Switzerland) started collecting data at Terceiro Jardim in Boa Viagem Beach over a shoreline length of 2.4 km and completed the survey at Boa Viagem Square within about 50 min.

Once the survey was completed, the roving receiver's data was downloaded, whereas the reference station's data were obtained from the IBGE website (IBGE 2017). The raw data were then processed using *Leica Geo Office* GNSS processing software. An elevation mask of 10° was adopted to reduce the effects of multipath and atmospheric errors.

RTK Method: Data Collection and Processing

Two Hiper Lite (Topcon Corporation, Tokyo) receivers were used, with one acting as a reference and the other as a roving receiver. The reference station was set at Terceiro Jardim (latitude 08° 06′ 30.16493″ S, longitude 34° 53′ 17.32463″ W, orthometric height 4.533 m, and ellipsoidal height −1.433 m). The station was on a benchmark, measuring 20 × 30 × 60 cm, with a metal sheet describing its identification. The roving receiver collected data in a *stop and go* mode, i.e., every 40 s it recorded data at points during the trajectory. An elevation mask of 10° was set. The RTK survey was performed on the same day as RK, with the roving receiver following the same shoreline track mapped by the receiver from RK. Both receivers logged data from the same satellites, as shown in Fig. 2(b).

PPP Method: Data Collection and Processing

For PPP, the data collected by the roving receiver during RK were treated as observable. To process this data, online freely available software provided by IBGE-PPP (IBGE 2017) was used. This service applies the Canadian Spatial Reference System (CSRS)-PPP program (GPS PPP) developed by the Geodetic Survey Division of Natural Resources of Canada (NRCan). It allows users with GNSS receivers to obtain coordinates in the official Brazilian datum called Geocentric Reference System for the Americas (SIRGAS 2000), which is tied to the International Terrestrial Reference Frame (ITRF). It uses the GNSS observation files from the users in RINEX or HATANAKA formats, and also makes use of other information, such as orbits and clocks (satellite), phase center correction of receiver's antennas, ITRF transformation parameters/SIRGAS 2000, ocean loading correction, velocity model, and the model of geoid undulation (*MAPGEO2010*). There are three types of precise orbits provided by NRCan, i.e., final, rapid, and ultrafast. The IBGE-PPP system uses the most accurate orbital available at the time of processing (e.g., final, rapid, ultrafast). In this work, the final orbital data were used and the service generated a report with the coordinates of the survey and its assessment of precision.

Evaluation Criteria

The evaluation criteria used to determine the shoreline's trajectory differences from the three GNSS methods was done using statistical samples between the shoreline cross sections of 5-m intervals between a reference line and the other three shorelines. The reference line was constructed using the baseline method (Leatherman and Clow 1983) and served as the starting point for all transects. It was manually established adjacent to the other shoreline positions using *ArcGIS* software. The remaining steps to get the shifts in each cross section to provide observations for statistical analysis were performed in the free extension digital shoreline analysis system (Thieler et al. 2009). To assess the methods, the following were computed.

1. Mean deviations from two shorelines, *slA* and *slB*, were computed as

$$\bar{x} = \frac{1}{n}\sum_{i=1}^{n}(slA_i - slB_i) \tag{1}$$

where $(slA_i - slB_i)$ = distance between the shorelines at the cross section; i and n = number of sections.

2. Standard deviation is obtained as

$$\sigma = \sqrt{\frac{1}{n-1}\sum_{i=1}^{n}(slA_i - slB_i - \bar{x})^2} \tag{2}$$

3. Root-mean-square error (RMSE) of the shoreline deviations are computed to gain a measure of the corresponding effectiveness of the methods. These were computed from

$$\text{RMSE} = \sqrt{\frac{1}{n-1}\sum_{i=1}^{n}(slA_i - slB_i)^2} \tag{3}$$

4. Minimum and maximum displacements between *slA* and *slB*.
5. Pearson correlation is used to give an indication of the similarity between the trajectories of the shorelines obtained from the three GNSS methods. It is computed as

$$r = \frac{n\left(\sum_{i=1}^{n} slA_i slB_i\right) - \left(\sum_{i=1}^{n} slA_i\right)\left(\sum_{i=1}^{n} slB_i\right)}{\sqrt{\left[n\sum_{i=1}^{n} slA_i^2 - \left(\sum_{i=1}^{n} slA_i\right)^2\right]\left[n\sum_{i=1}^{n} slB_i^2 - \left(\sum_{i=1}^{n} slB_i\right)^2\right]}} \tag{4}$$

6. Coordinate precision (planimetric and altimetric) was obtained for each method using the following statistics: arithmetic mean, standard deviation, and minimum and maximum precision reached.

Results and Discussions

Results

Table 1 shows the volume of shoreline data collected (i.e., the amount of points generated) by each method. The length covered by the methods was 2.4 km, with a time interval of 50 min reaching an average velocity of 2.9 km/h.

Table 2. Statistics for the Three Methods

Method	$\bar{x}$ (m) (planimetric precision)	x(m) (altimetric precision)	σ (m) (planimetric precision)	σ (m) (altimetric precision)	Maximum (m) (value of planimetric precision)	Minimum (m) (value of planimetric precision)
slRTK	0.01	0.01	0.01	0.01	0.05	0.01
slRK	0.07	0.11	0.06	0.08	0.24	0.01
slPPP	0.27	0.42	0.08	0.08	0.49	0.19

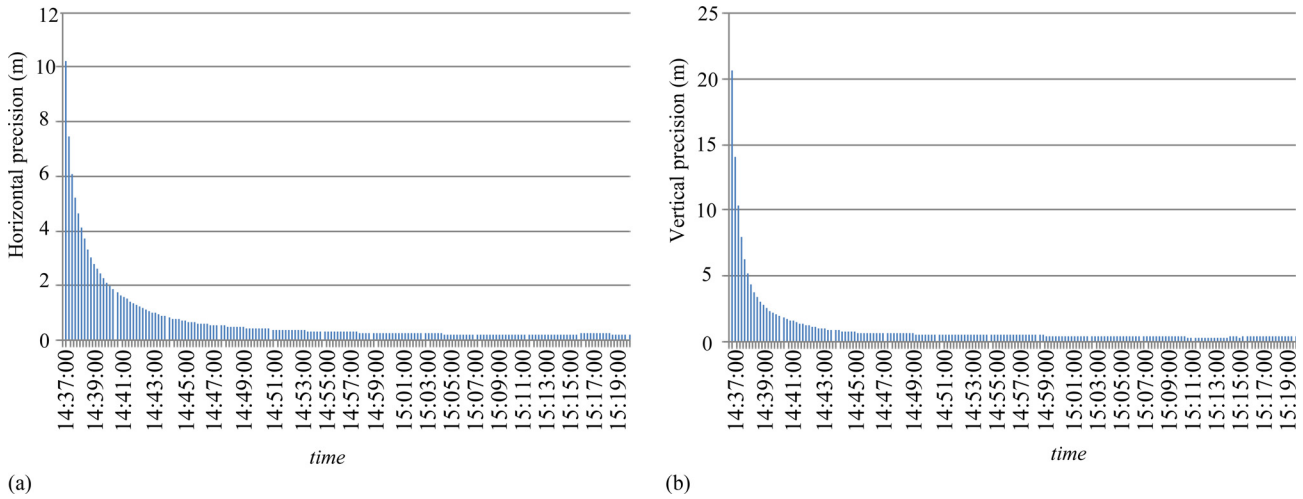

Fig. 6: PPP during time survey: (a) horizontal precision; (b) vertical precision

In Table 2, four evaluation criteria ($\bar{x}$, σ, and maximum and minimum values) based on planimetric and altimetric precision obtained by the three GNSS methods are presented. This information is normally provided as a report after postprocessing of the data with the coordinates for each point or determined (*slRTK*) for each point during the RTK survey in real time. Both are provided by the GNSS commercial software while processing or extracting the data. This assessment shows that the *slRTK* method has less variability of precision reaching the centimeter level, i.e., $\bar{x} = 1$ cm with $\sigma = \pm 1$ cm, followed by *slRK* $\bar{x} = 7$ cm with $\sigma = \pm 6$ cm, and $\bar{x} = 27$ cm with $\sigma = \pm 42$ cm for *slPPP*. However, the precision of the methods must be interpreted with caution because standard errors of GNSS measurements tend to be overambitious in practice. Therefore, it is not possible to estimate the level of accuracy reached by each method based on standard deviations alone. Further analysis was therefore undertaken.

In Figs. 6(a and b), the *time* and *precision* (horizontal and vertical) obtained from the *slPPP* method are presented. In this method it is possible to visualize that it takes around 10 min to get a stable precision (horizontal and vertical). These starting minutes were not computed during the statistical analysis. It is also important to note that before the start of the survey, after initializing the receiver, a period of 10–20 min is necessary for stabilization. This is recommended for all the three methods.

The shoreline shift differences ($slA_i - slB_i$) were performed based on a combinatorial approach (i.e., relative comparison) by choosing combinations among the three methods ($slRTK_i - slRK_i$), ($slRTK_i - slPPP_i$), and ($slRK_i - slPPP_i$) according to Evaluation Criteria 1–5. Fig. 7 shows an example of the shorelines and cross sections. The results in Table 3 show this comparison between the shorelines. For the 453 samples, the mean shift

Fig. 7: Transects of 5-m intervals of sampling to verify the difference between the trajectories (background satellite image © 2017 DigitalGlobe; supported by FACEPE/CNPq Grant No. PPP/APQ-1242-1.07/10)

difference for $(slRTK_i - slRK_i)$ was $\bar{x} = 63$ cm with $\sigma = \pm 46$ cm and RMSE = 78 cm. When compared with $(slRTK_i - slPPP_i)$ the results are $\bar{x} = 64$ cm with $\sigma = \pm 48$ cm and RMSE = 80 cm, and compared with the difference between relative $(slRK_i - slPPP_i)$, $\bar{x} = 9$ cm with $\sigma = \pm 15$ cm and RMSE = 17 cm. Also, it was possible to evaluate the Pearson correlation according to Eq. (4), yielding 99.97, 99.96, and 99.99% of correlation among (*slRTK* and *slRK*), (*slRTK* and *slPPP*), and (*slRK* and *slPPP*), respectively.

Analysis of the Results

One important criteria when using GNSS for shoreline monitoring is to use the same method as well as the same receiver during the campaigns to avoid systematic errors. Another point to highlight for managers is to check the appropriate datum and geodetic system as well as to verify if the coordinates used for relative positioning are in the same ITRF epoch (Howfman-Wellenhof et al. 2008; Leick 2004).

The *slRTK* method provided the best results concerning point precision (Table 2); however, when compared with the shoreline obtained by *slPPP* and *slRK*, a mean difference between them of around 64 cm shown in Table 3 was found. In this experiment, the idea was to use the conditions that the site provided as a practical monitoring scenario, i.e., using the stations available in the case of RBMC for processing RK and municipality information on points with known coordinates.

The RTK method has some limitations due to the radio signal transmission range between the base station and rover receiver. It is well known that, the connection can work properly for approximately 10 km between rover and base. In this survey, the connection presented losses of signal at about 2 km due to the combination of obstructions in the area, such as tall buildings, kiosks, and trees, together with the natural slope of the region. This limitation disqualifies this method for mapping the shoreline of a state like Pernambuco, which has an extension of 187 km. Also, it will be necessary to have a consolidated coastal geodetic network to cover the entire State of Pernambuco with points in the same reference frame every 5 km to support the base stations while using the RTK method. This is, however, not reliable and cost-effective.

The RK method is also dependent on the base station distance to process the results. If the distance is shorter, better results are expected. For this study, the base station used to process the data was around 10 km away from the roving receiver. Accordingly, with few permanent stations covering the State of Pernambuco, even considering available stations from neighboring states that are hundreds of kilometers away could pose a challenge for practical surveys.

The Pearson correlation showed a very strong correlation between the RK and PPP shorelines (99.99%) (Table 3). For practical applications, therefore, they can be assumed to be the same. The main advantage of PPP, however, is the use of a single GNSS receiver, thus, saving on instrument and manpower-related costs.

Considering the uncertainty associated with the field crew's visual estimation of the shoreline position of up to about 1 m depending on a number of factors, e.g., beach types and the experience level of the field crew, all the previously mentioned assessed methods could be used for shoreline monitoring. In this regard, for a given shoreline monitoring project, one would recommend the use of the method that is easiest and cheapest. In summary, all shoreline methods could be recommended for CZM offices; however, it is important to highlight the advantages of each one, as shown by the experiment in Table 4.

Objective 4 of this study was to provide guidance for choosing the most appropriate and economically viable technique for mapping the Pernambuco State shoreline, with an extension of about 200 km. From the results in Tables 3 and 4, the kinematic PPP method presented the best alternative for this purpose considering the characteristics of the GNSS network for this site. For this particular case without cliffs along the shoreline, the kinematic trajectory could be performed reliably using, e.g., all-terrain vehicles, whereas the GNSS antenna is normally mounted into a vehicle. In cases of with path obstructions, the survey could be covered on foot. Generally, looking at the legislation of Article 10 governing the Pernambuco policy, all of the three GNSS methods discussed earlier could in principle support it; however, some of them would not be realistic considering the peculiarities cited earlier.

Conclusion

This study evaluated three commonly used GNSS methods that support shoreline mapping, i.e., RK, RTK, and PPP. There are many issues that should be considered when choosing a method for mapping positional variations of shoreline that are particularly

Table 3. Transects and Statistics

Method	$slRTK_i - slRK_i$	$slRTK_i - slPPP_i$	$slRK_i - slPPP_i$
Number of transects (samples)	453	453	453
$\bar{x}$ (m)	0.63	0.64	0.09
σ (m)	0.46	0.48	0.15
RMSE (m)	0.78	0.80	0.17
Maximum shift (m)	2.71	3.05	2.24
Minimum shift (m)	0.01	0.00	0.00
Pearson correlation	0.9997 (99.97%)	0.9996 (99.96%)	0.9999 (99.99%)

Table 4. Summary of the Field Application of the Three GNSS Methods

Shoreline method	RTK	RK	PPP
Number of receivers	2	2	1
Needs postprocessing	No	Yes	Yes
Needs of a base station	Yes	Yes	No
Distance between rover and base station	Limited by the radio range	Closer is better	Not applied

applicable to the State of Pernambuco to support ICZM policies. Considerations include the use of a shoreline indicator and how to map and monitor it. From the evaluation of GNSS-based shoreline monitoring methods based on the case study of Pernambuco, the result of this evaluation indicated the following:

1. Using statistics considering the shoreline planimetric and altimetric precision regarding the mean ($\bar{x}$) and standard deviation (σ) for the three methods, the resulting planimetric precisions (in meters) are *slRTK* ($\bar{x}$) 0.01, (σ) 0.01; *slRK* ($\bar{x}$) 0.07, (σ) 0.06; and *slPPP* ($\bar{x}$) 0.27, (σ) 0.08. The results found for altimetric precision (in meters) are *slRTK* ($\bar{x}$) 0.01, (σ) 0.01; *slRK* ($\bar{x}$) 0.11, (σ) 0.08; and *slPPP* ($\bar{x}$) 0.42, (σ) 0.08. These results provide quality and quantitative indicatives of the methods. However, alone, they do not provide enough information for managers to make the best choice when selecting a method for shoreline surveys.
2. Comparing the trajectory of the shorelines $(slRTK_i - slRK_i)$, $(slRTK_i - slPPP_i)$, and $(slRK_i - slPPP_i)$ resulted in ($\bar{x}$) 0.63 m, (σ) 0.46 m; ($\bar{x}$) 0.64 m, (σ) 0.48 m; and ($\bar{x}$) 0.09 m, (σ) 0.15 m, respectively. The results found by the GNSS-based evaluation provided a strong correlation when comparing *slPPP* with *slRTK* (99.97%) and *slPPP* with *slRK* (99.99%). These statistics show the main results for a relative comparison between the shoreline trajectories obtained by each method and highlight the fact that other criteria should be analyzed to address the concerns of the ICMZ of Pernambuco State. Among these concerns are the extent of the state's GNSS network configuration, which does not provide ideal short baselines to support RTK and RK, and the lack of benchmarks in the survey area due to the low geographical density of stations belonging to the network.
3. The choice of a particular GNSS method is very important for an efficient and reliable shoreline monitoring. In this evaluation the PPP method is considered to be both economical and feasible for the case study and shown to be a reliable alternative for mapping and monitoring of shoreline that could be used to support the Pernambuco legislation presented in Article 10.

Future works will analyze the behavior of PPP in tracking long shoreline distances (e.g., 200 km) and consider the removal of outliers in postprocessed data.

Acknowledgments

The first author acknowledges the financial support of the Post-Doctoral CNPq scholarship (233170/2013-8) that supported his stay at Curtin University, Australia, and the support of CNPq Grant 310412/2015-3/PQ level 2. The authors are also grateful for the Brazilian Science without Borders Program/CAPES Grant 88881.068057/2014-01, which supported Dr. Awange's stay at the UFPE, Brazil.

References

Abbott, T. (2013). "Shifting shorelines and political winds The complexities of implementing the simple idea of shoreline setbacks for oceanfront developments in Maui, Hawaii." *Ocean Coastal Manage.*, 73, 13–21.

ArcGIS [Computer software]. Esri, Redlands, CA.

Awange, J. L. (2012). *Environmental monitoring using GNSS Global Navigations Satellite Systems*, Springer, New York, 382.

Baldock, J., Bancroft, K. P., Williams, M., Shedrawi, G., and Field. S. (2014). "Accurately estimating local water temperature from remotely sensed satellite sea surface temperature: A near real-time monitoring tool for marine protected areas." *Ocean Coastal Manage.*, 96, 73–81.

Boak, E. H., and Turner, I. L. (2005). "Shoreline definition and detection: A review." *J. Coastal Res.*, 21(4), 688–703.

Botero, C., Pereira, C., Tosic, M., and Manjarrez, G. (2015). "Design of an index for monitoring the environmental quality of tourist beaches from a holistic approach." *Ocean Coastal Manage.*, 108, 65–73.

Clarck, J. R. (1992). "Integrated management of coastal zones." ⟨http://www.fao.org/docrep/003/T0708E/T0708E00.htm#TOC⟩ (Jun. 24, 2013).

Dibajnia, M., Soltanpour, M., Vafai, F., Shoushtari, S. M. H. J., and Kebriaee, A. (2012). "A shoreline management plan for Iranian coastlines." *Ocean Coastal Manage.*, 63, 1–15.

Dolan, R., and Heywood, J. (1976). "Landsat application of remote sensing to shoreline-form analysis." *NASA Technical Rep.*, Goddard Space Flight Center, Greenbelt, MD, 33.

Dominguez, J. M. L., Bittencourt, A. C. S. P., Leao, Z. M. A. N., and Azevedo, A. E. G. (1990). "Geologia do quaternário costeiro do Estado de Pernambuco." *Rev. Bras. Geocin.*, 20, 208–215.

Dugan, J. P., Morris, W. D., Vierra, K. C., Piotrowski, C. C., Farruggia, G. J., and Campion, D. C. (2001). "Jetski-based nearshore bathymetric and current survey system." *J. Coastal Res.*, 17(4), 900–908.

El-Rabbany, A. (2006). *Introduction to GPS: The global positioning system*, 2nd Ed., Artech House, Boston.

Gao, Y. (2006). "Precise point positioning and its challenges." Inside GNSS, Nov/Dec, 1618.

Genz, A. S., Frazer, L. N., and Fletcher, C. H. (2009). "Toward parsimony in shoreline change prediction (II): Applying basis function methods to real and synthetic data." *J. Coastal Res.*, 25(2), 380–392.

Goncalves, R. M., Awange, J., and Krueger, C. P. (2012a). "GNSS-based monitoring and mapping of shoreline position in support of planning and management of Matinhos/PR (Brazil)." *J. Global Positioning Syst.*, 11, 156–168.

Goncalves, R. M., Awange, J., Krueger, C. P., Heck, B., and Coelho, L. S. (2012b). "A comparison between three short-term shoreline prediction models." *Ocean Coastal Manage.*, 69, 102–110.

Graham, D., Sault, M., and Bailey, J. (2003). "National Ocean Service shoreline: Past, present, and future." *Shoreline mapping and change analysis: Technical considerations and management implications*, M. Byrnes, M. Crowell, and C. Fowler, (eds.), *J. Coastal Res.*, 38, 14–32.

Howfman-Wellenhof, B., Lichtenegger, H., and Wasle, E. (2008). *GNSS global navigation satellite system: GPS, GLONASS, Galileo and more*, Springer, Wien.

IBGE (Brazilian Institute of Geography and Statistics). (2010). "Population distribution map 2000." ⟨http://www.ibge.gov.br/home/geociencias/geografia/mapas_doc1.shtm⟩ (Jul. 13, 2012).

IBGE (Brazilian Institute of Geography and Statistics). (2017). "Precision point positioning (PPP)." ⟨http://www.ppp.ibge.gov.br/ppp.htm⟩ (Nov. 17, 2015).

Jacobson, C., Carter, R. W., Thomsen, D. C., and Smith, T. F. (2014). "Monitoring and evaluation for adaptive coastal management." *Ocean Coastal Manage.*, 89, 51–57.

Juan, J. M., et al. (2012). "Enhanced precise point positioning for GNSS users." *IEEE Trans. Geosci. Remote Sens.*, 50(10), 4213–22.

Lawrence, P. L. (1995). "Development of Great Lakes shoreline management plans by Ontario conservation authorities." *Ocean Coastal Manage.*, 26(3), 205–223.

Leandro, R. F., Santos, M. C., and Langley, R. B. (2011). "Analyzing GNSS data in precise point positioning software." *GPS Solutions*, 15(1), 1–13.

Leatherman, S. P., and Clow, J. B. (1983). "UMD shoreline mapping project." *IEEE Geosci Remote Sens. Soc. Newsl.*, 22, 5–8.

Leick, A. (2004). *GPS satellite surveying*, 3rd. Ed., John Wiley, Hoboken, NJ, 435.

Leica Geo Office [Computer software]. Leica Geosystems AG, St. Gallen, Switzerland.

Li, P., and Zhang, X. (2014). "Integrating GPS and GLONASS to accelerate convergence and initialization times of precise point positioning." *GPS Solutions*, 18(3), 461–471.

Mallmann, D. L. B., Araujo, T. C. M., and Droguett, E. L. (2014). "Characterization of central coast of Pernambuco State (Brazil)

regarding to short and medium-term erosion." *Quat. Environ. Geosci.*, 5(2), 137–154.
Mancini, F., Dubbini, M., Gattelli, M., Stecchi, F., Fabbri, S., and Gabbianelli, G. (2013). "Using unmanned aerial vehicles (UAV) for high-resolution reconstruction of topography: The structure from motion approach on coastal environments." *Remote Sens.*, 5(12), 6880–6898.
Manso, V. A., Coutinho, P. N., Guerra N. C., and, Soares, Jr., C. F. A. (2006). *Eroso e prograd ao do litoral brasileiro*, Ministrio do Meio Ambiente, Brasilia, Brazil, 179–196.
MAPGEO2010 [Computer software]. IBGE, Rio de Janeiro, Brazil.
Mendonça, F. J. B., Gonçalves, R. M., Awange, J., Silva, L. M., and Gregório, M. N. (2014). "Temporal shoreline series analysis using GNSS." *Bol. Ciênc. Geod.*, 20(3), 701–719.
Muehe, D. (2006). *Erosao e progradacao do litoral brasileiro*, Ministerio do Meio Ambiente, Brasilia, Brazil, 476.
National Oceanic and Atmospheric Administration (NOAA). (2017). "Coastal mapping program." ⟨http://www.ngs.noaa.gov/RSD/cmp.shtml⟩ (Jun. 21, 2015).
Parrish, C. E. (2012). "Shoreline mapping." *Advances in mapping from remote sensor imagery: Techniques and applications*, X. Yang and J. Li, eds., CRC/Taylor & Francis Group, Boca Raton, FL, 145–168.
Parrish, C. E., Sault, M., White, S. A. and Sellars, J. (2005). "Empirical analysis of aerial camera filters for shoreline mapping." *Proc., American Society for Photogrammetry and Remote Sensing Annual Conf.*, American Society for Photogrammetry and Remote Sensing, Bethesda, MD, 1–11.
Portz, L., Manzolli, R. P., Hermanns, L., and Alcantara Carrió, J. (2015). "Evaluation of the efficiency of dune reconstruction techniques in Xangri-la (Rio Grande do Sul, Brazil)." *Ocean Coastal Manage.*, 104, 78–89.
Pugh, D. T. (1987). *Tides, surges and mean sea level*, John Wiley, New York, 472.
Smith, J. T., Jr. (1981). *A history of flying and photography in the photogrammetry division of the national ocean survey, 1919–79*, U.S. Dept. of Commerce, National Oceanic and Atmospheric Administration, National Ocean Service, Silver Spring, MD, 486.
Souza, C. R. G. (2009). "Coastal erosion and the coastal zone management challenges in Brazil." *J. Integr. Coastal Zone Manage.*, 9(1), 17–37.
Stockdon, H. F., Sallenger, A. H., Jr., List, J. H., and Holman, R. A. (2002). "Estimation of shoreline position and change using airborne topographic lidar data." *J. Coastal Res.*, 18(3), 502–513.
Thieler, E. R., Himmelstoss, E. A., Zichichi, J. L., and Ergul, A. (2009). "Digital shoreline analysis system (DSAS) version 4.0–An ArcGIS extension for calculating shoreline change." *USGS Open-File Rep. 2008-1278*, Washington, DC.
Westoby, M. J., Brasington, J., Glasser, N. F., Hambrey, M. J., and Reynolds, J. M. (2012). "'Structure-from-Motion' photogrammetry: A low-cost, effective tool for geoscience applications." *Geomorphology*, 179, 300–314.
White, S. A., Parrish, C. E., Calder, B. R., Pe'eri, S., and Rzhanov, Y. (2011). "Lidar-derived national shoreline: Empirical and stochastic uncertainty analyses." *J. Coastal Res.*, 62, 62–74.
Yao, F., Parrish, C. E., Pe'eri, S., Calder, B. R., and Rzhanov, Y. (2015). "Modeling uncertainty in photogrammetry-derived national shoreline." *Mar. Geod.*, 38(2), 128–145.